TRANSPORT

- Mass Transport $J = -D\, dC/dx$ (Fick's Law)
- Heat Transport $Q = -k\, dT/dx$ (Fourier's Law)
- Momentum Transport $\tau = -\mu\, dv/dy$ (Newton's Law)

- Charge Transport $V = IR$

$$J = \sigma E = \sigma\, dV/dx$$

$$J_{Ay}^{*} = -D_{AB}\frac{dc_A}{dy}$$

$$D = D_0 \exp(-E_a / RT)$$

$$\frac{\partial c}{\partial t} = \frac{\partial}{\partial x}\left(D\frac{\partial c}{\partial x}\right)$$

$$\frac{\partial c}{\partial t} = D\frac{\partial^2 c}{\partial x^2}$$

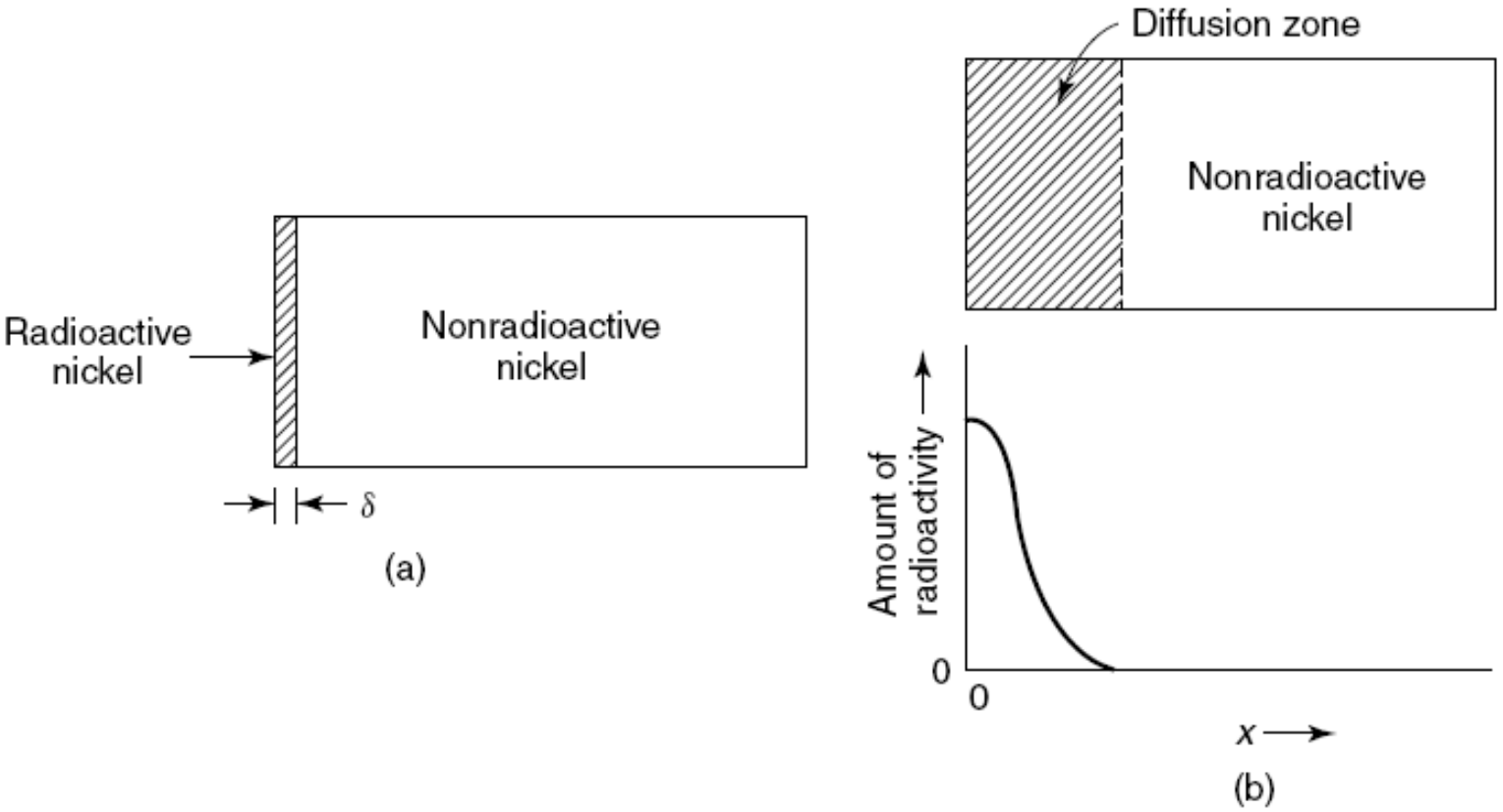

Figure 4.38 Schematic illustration of a self-diffusion experiment in which (a) a thin layer of radioactive nickel is deposited on one surface of a nonradioactive nickel specimen. After heating and time (b), the radioactive nickel has diffused into the sample, as monitored with a radioactive detector. From K. M. Ralls, T. H. Courtney, and J. Wulff, *Introduction to Materials Science and Engineering*. Copyright © 1976 by John Wiley & Sons, Inc. This material is used by permission John Wiley & Sons, Inc.

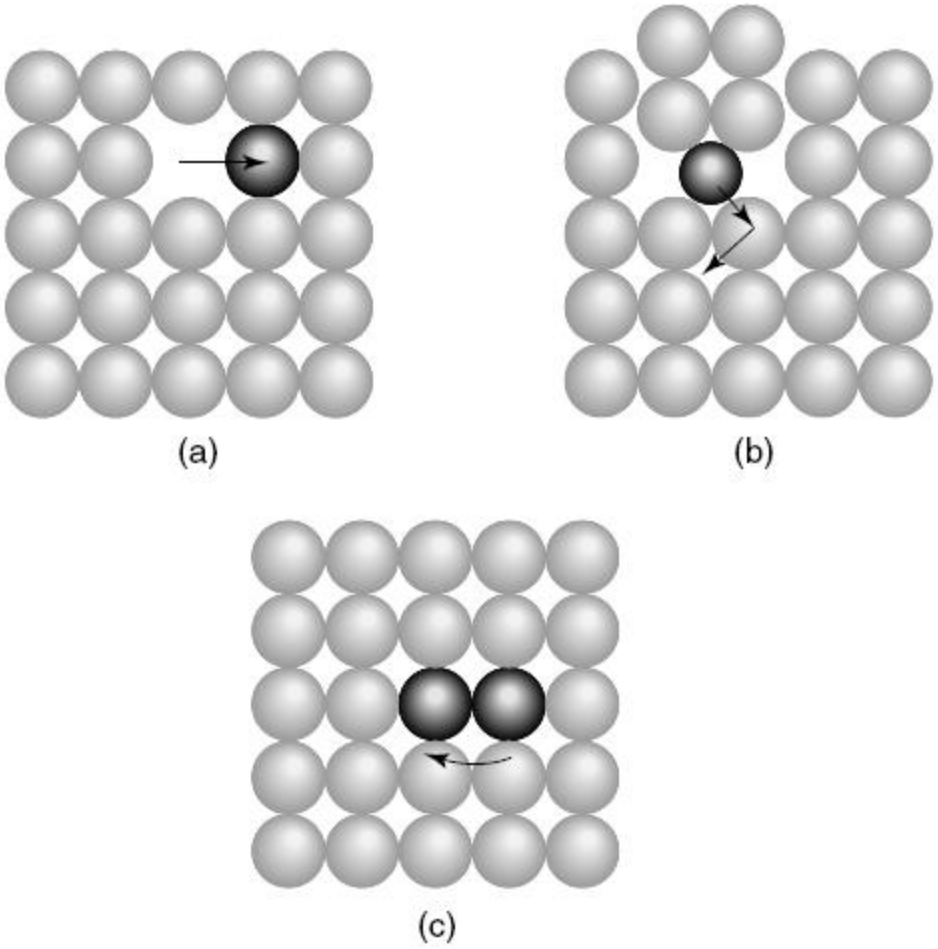

Figure 4.39 Illustration of (a) vacancy, (b) interstitial, and (c) interchange (exchange) mechanisms in atomic diffusion. From K. M. Ralls, T. H. Courtney, and J. Wulff, *Introduction to Materials Science and Engineering*. Copyright © 1976 by John Wiley & Sons, Inc. This material is used by permission John Wiley & Sons, Inc.

Table 4.16 Frequency Factors, Activation Energies and Melting Points for Self-Diffusion in Selected Metals

Species	D_0 (cm^2/s)	E_a (KJ/mol)	T_m (°C)
Pb	6.6	117	327
Zn (‖ to c axis)	0.046	85	419
Zn (⊥ to c axis)	91	130	419
Ag	0.89	192	962
Au	0.16	222	1064
Cu	11	239	1085
Ni	—	293	1455
Co	0.31	280	1494
α-Fe	2300	306	1538
γ-Fe	5.8	310	—
Pt	0.048	233	1772

Source: B. Chalmers, *Physical Metallurgy*. Copyright © 1959 by John Wiley & Sons, Inc.

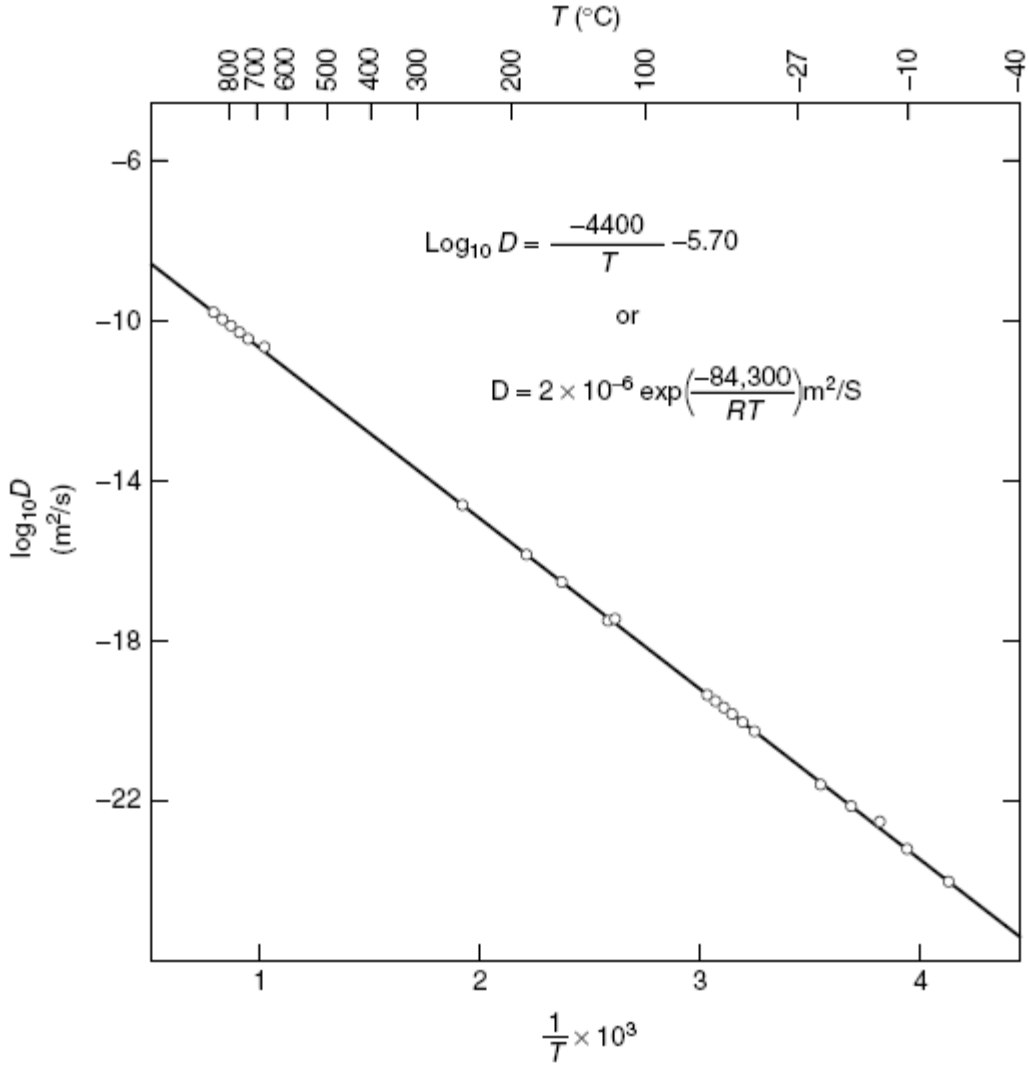

Figure 4.41 Variation with temperature of the diffusivity for carbon in BCC-Fe (α – Fe). Activation energy is in units of J/mol. Reprinted, by permission, from D. R. Gaskell, *An Introduction to Transport Phenomena in Materials Engineering*, p. 519. Copyright © 1992 by Macmillan Publishing Co.

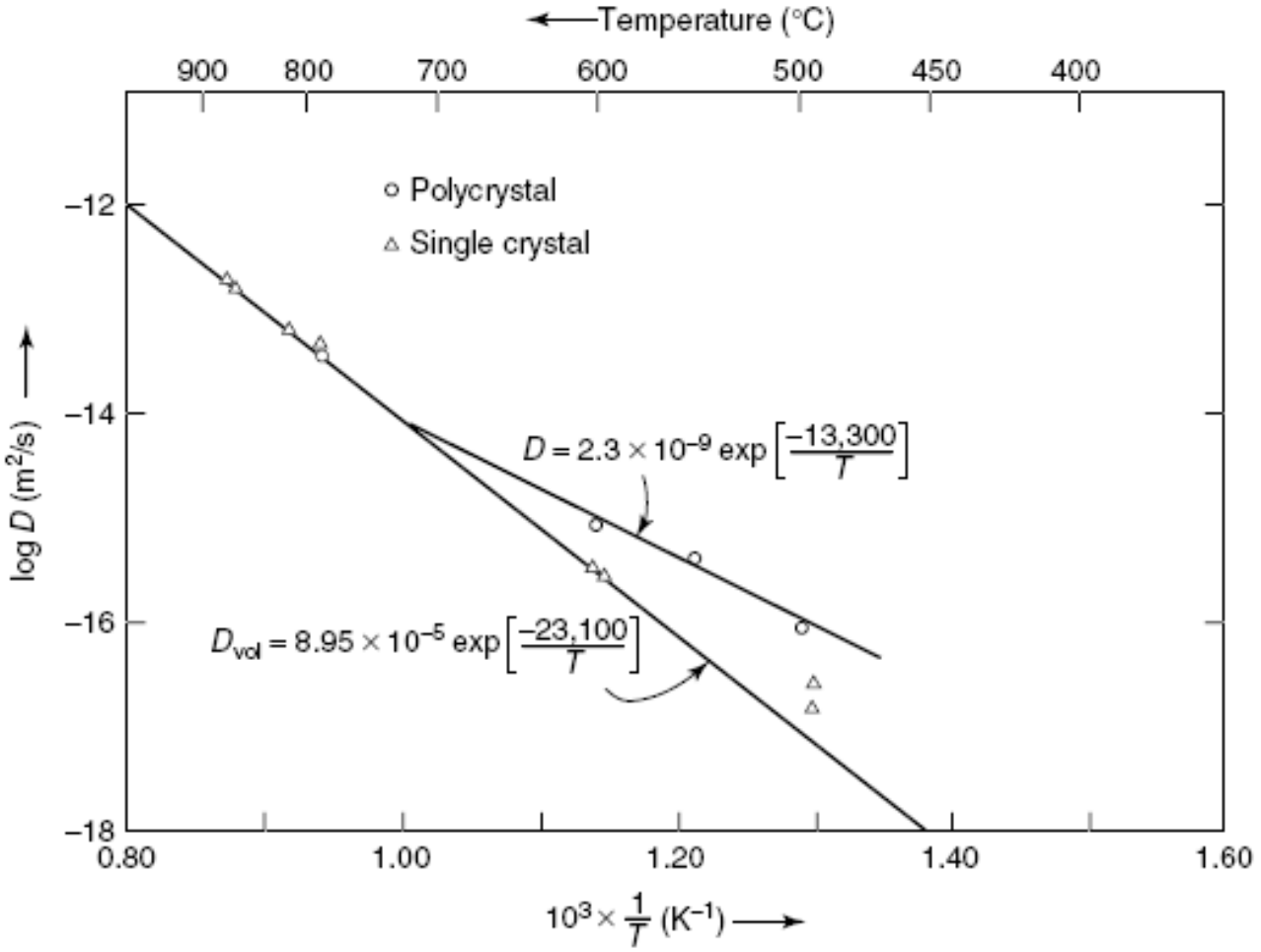

Figure 4.42 Self-diffusion coefficient in single and polycrystalline silver, illustrating the effect of grain boundary diffusion, especially at lower temperatures. From K. M. Ralls, T. H. Courtney, and J. Wulff, *Introduction to Materials Science and Engineering*. Copyright © 1976 by John Wiley & Sons, Inc. This material is used by permission John Wiley & Sons, Inc.

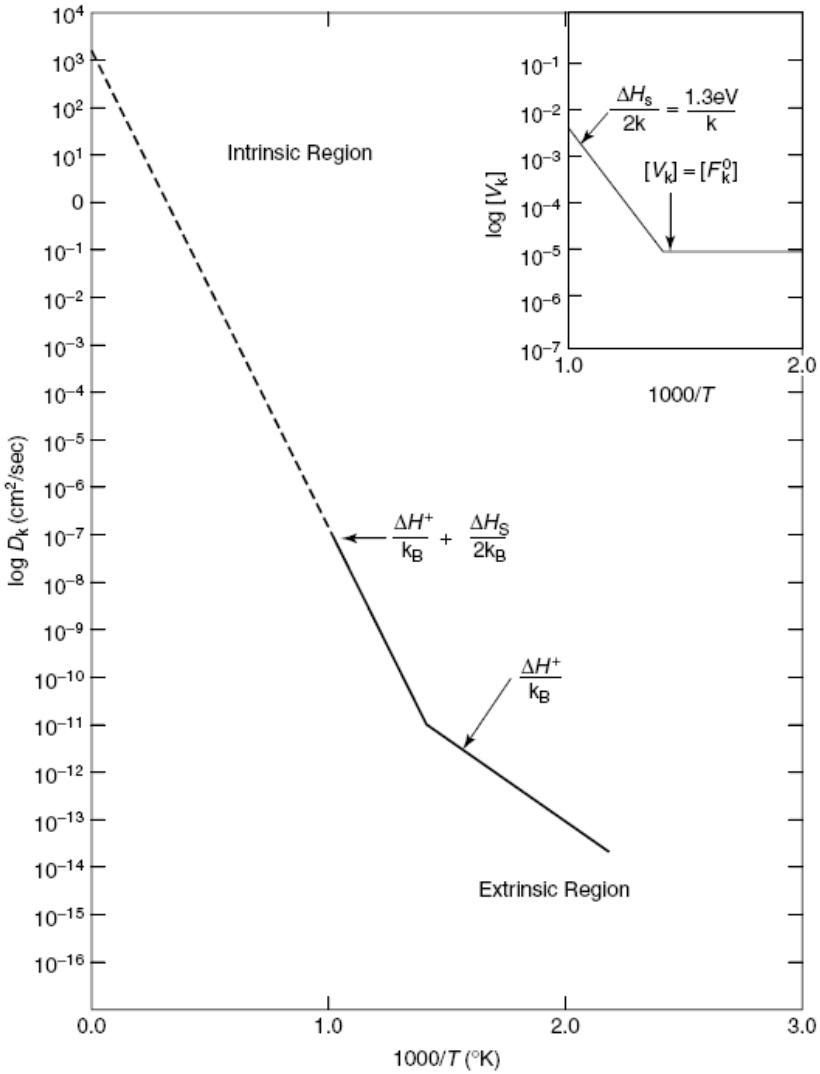

Figure 4.44 Diffusivity as a function of temperature for KC1 with 10^{-5} atom fraction divalent cation impurities. Insert plot shows the variation of vacancies with temperature. Adapted from W. D. Kingery, H. K. Bowen, and D. R. Uhlmann, *Introduction to Ceramics*. Copyright © 1976 by John Wiley & Sons, Inc. This material is used by permission of John Wiley & Sons, Inc.

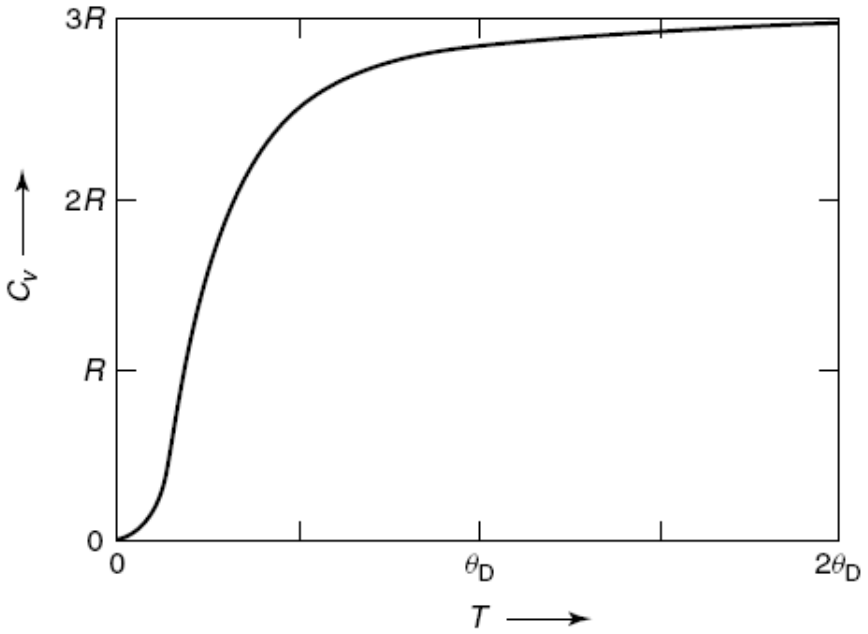

Figure 4.24 Molar heat capacity as a function of temperature, based on the Debye model. From K. M. Ralls, T. H. Courtney, and J. Wulff, *Introduction to Materials Science and Engineering*. Copyright © 1976 by John Wiley & Sons, Inc. This material is used by permission John Wiley & Sons, Inc.

$$C_{vl} = \frac{12\pi^4 R}{5}\left(\frac{T}{\theta_D}\right)^3$$

$$C_{ve} = \frac{\pi^2 n k_B^2 T}{2E_F}$$

$$C_v = C_{vl} + C_{ve} = \alpha T^3 + \gamma T$$

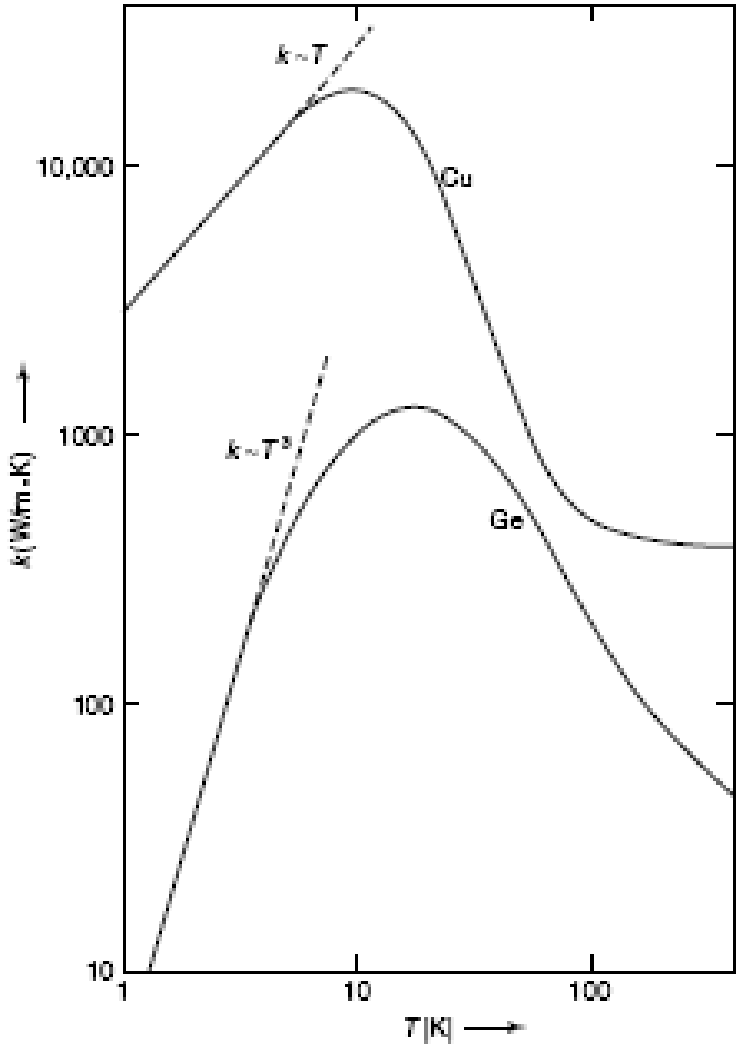

Figure 4.25 Temperature dependence of thermal conductivity for a pure metal (Cu) and a non-metal (Ge), illustrating different temperature dependences at low temperature. From K. M. Ralls, T. H. Courtney, and J. Wulff, *Introduction to Materials Science and Engineering*. Copyright © 1976 by John Wiley & Sons, Inc. This material is used by permission John Wiley & Sons, Inc.

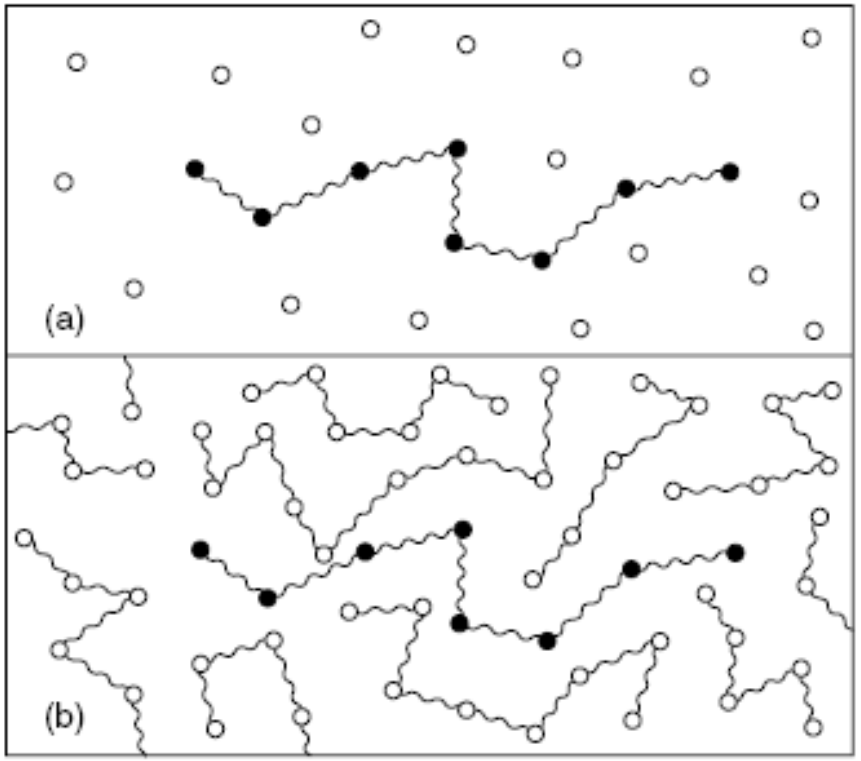

Figure 4.52 Single-molecule bead spring models for (a) dilute polymer solution and (b) polymer melt. From R. B. Bird, W. E. Stewart, and E. N. Lightfoot, *Transport Phenomena*, 2nd ed. Copyright © 2002 by John Wiley & Sons, Inc. This material is used by permission of John Wiley & Sons, Inc.

Figure 4.53 Schematic illustration of the reptation process in polymer melts, showing chain entanglements (light arrows), the "wriggling motion" of the polymer chain (darker arrows), and the primitive path of the polymer chain (dark line). Reprinted, by permission, from G. Strobl, *The Physics of Polymers*, 2nd ed., p. 283. Copyright © 1997 by Springer-Verlag.

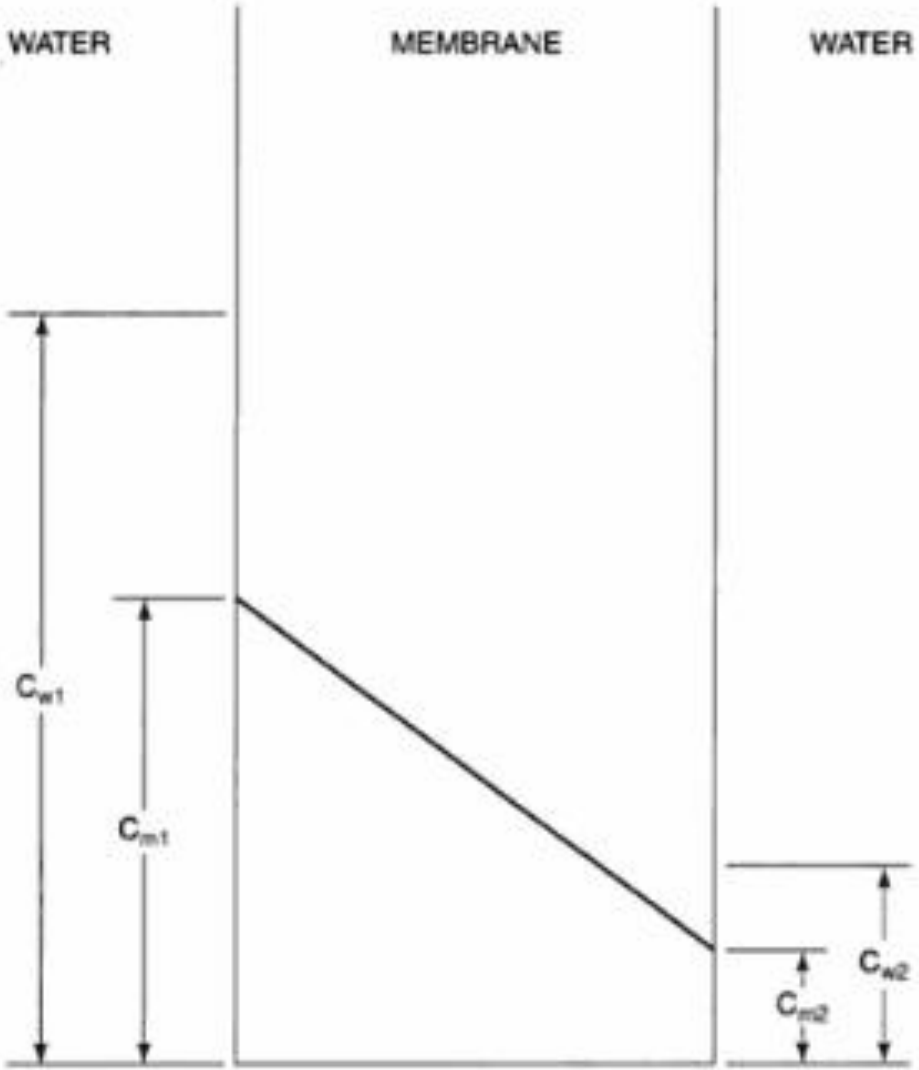

Figure 4.55 Schematic illustration of concentration drop at a membrane interface, and concentration gradient across the membrane. From A. T. Johnson, *Biological Process Engineering*. Copyright © 1999 by John Wiley & Sons, Inc. This material is used by permission of John Wiley & Sons, Inc.

Table 4.17 Permeabilities of Selected Polymers

Film Type	Permeability [10^{15} $m^4/(s\ N)$]		
	Oxygen	Carbon Dioxide	Water Vapor
Low-density polyethylene	0.45–1.5	0.88–8.8	0.97–3.8
Linear low-density polyethylene	0.80–1.1	—	2.6–5.0
Medium-density polyethylene	0.30–0.95	0.88–4.4	1.3–2.4
High-density polyethylene	0.059–0.46	0.45–1.1	0.65–1.6
Polypropylene	0.15–0.73	0.88–2.4	0.65–1.7
Polyvinyl chloride	0.071–0.26	0.49–0.93	—
Polyvinyl chloride, plasticized	0.0088–0.086	0.088–6.3	>1.3
Polystyrene	0.023–0.088	1.1–3.0	18–25
Ethylene vinyl acetate copolymer (12%)	0.091–1.5	4.0–6.1	9.7
Ionomer	0.40–0.86	1.1–2.0	3.6–4.9
Ruber hydrochloride	0.015–0.15	0.059–0.59	>1.3
Polyvinylidene chloride	0.00091–0.0030	0.0067	0.24–0.81

Source: A. T. Johnson, *Biological Process Engineering*.